Original
Received January 18, 2006
Accepted for Publication April 3, 2006

Chemical Composition of Advanced Materials as Obtained by the 3-Dimensional Atom Probe

Reiner KIRCHHEIM

Institut für Materialphysik, University of Göttingen,
Friedrich-Hund-Platz 1, D-37077 Göttingen, Germany
E-mail : rkirch@ump.gwdg.de

The 3-dimensional atom probe is based on field ion microscopy where the screen is replaced by a 2-dimensional, position sensitive detector. Atoms were removed from a conducting sample by a high voltage pulse. The time of flight reveals their chemical nature, and continuous stripping allows lateral and in-depth analysis. The spatial resolution permits a chemical analysis on the sub-nanometer scale. Results of this new technique are presented for (i) the initial stages of interdiffusion at the boundary between two metals, (ii) P-segregation at grain boundaries in nanocrystalline Ni-P alloys, (iii) initial stages of nucleation and growth in various alloys, (iv) composition of thin oxide films in TMR-structures, and (v) distribution of hydrogen in metallic multilayers. It will be also shown that the new technique not only allowed a characterization on the atomic scale but verified and/or falsified existing models for the examples given before.

Key Words : atom probe, nanostructures, TMR-structures

1 INTRODUCTION

The purpose of the present paper is to summarize recent results which were obtained by a 3-dimensional or tomographic atom probe (Refs. [1, 2]). It is based on field ion microscopy where the screen is replaced by a 2-dimensional, position sensitive detector. Thus the lateral coordinates of atoms which were removed from a conducting sample by a high voltage pulse can be determined. The time of flight reveals their chemical nature, and continuous stripping allows in-depth analysis. In order to obtain the necessary electric fields for removing and ionizing atoms, the sample has to be prepared as a tip with a radius of curvature which is less than 50 nm. This analytical tool has been available for about two decades and it provides data about the chemical nature of atoms and their position within a typical volume of $15 \times 15 \times 100$ nm with a lateral resolution of about 0.3 nm and a depth resolution of better than 0.1 nm. Thus dense packed lattice planes are often resolved by the technique as shown in Figure 1.

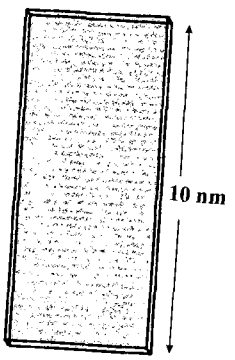

Figure 1 Positions of Ag-atoms in Ag-sample revealing dense packed (111)-planes

Compared to other techniques with atomic resolution like high resolution transmission electron microscopy (HREM) and/or scanning tunnelling microscopy (STM) the atom probe yields real 3-dimensional data and quantitative results regarding the chemical composition of a sample. This advantage is counteracted by the difficult sample preparation and the limitation of conducting, i.e. metallic, samples. With the availability of dual beam focussed ion beams the matter of preparing tip shaped sample has become much easier.

2 RESULTS AND DISCUSSION

2.1 Nucleation and growth

The tomographic atom probe allows determining the composition of nuclei as small as 1 nm in diameter. An example is shown in Figure 2 for a Cu-0.7 at.-% Fe alloy which was quenched into a homogeneous state and then annealed 803 K for 5 min (for details see Ref. [3]). At this temperature the Fe-content is above the solubility and according to the phase diagram and the classical nucleation theory a nucleus with a composition close to pure iron should form. However, there are regions in the sample where the composition is much smaller (cf. Figure 2). At the initial stage of nucleation the precipitates are usually coherent which can be revealed in some favourite cases as presented in Figure 3 for a

Cu-0.7 at.-% Ti alloy annealed at 623 K for 30 days (Ref. [4]). This sample formed Cu_3Ti precipitates in agreement with the phase diagram. The morphology of the precipitates is immediately obvious in an atom probe analysis as shown in Figure 4 for a Cu-Be alloy. A striking example of morphological changes has been shown for the first time by the atom probe in the Cu-Co system (Ref. [5] and Figure 5). Despite numerous investigations conducted on the Cu-Co system, motivated by its interesting magnetic properties, the formation of cylindrically shaped Co-precipitates was overlooked. One reason for this may be that the contrast of Cu and Co is very weak in HREM. In addition, the cigar shaped Co-particles form in narrow windows of annealing time and temperature only. It was shown in Ref. [5] that the long axis of the precipitates is in the mechanically soft [110] direction. A detailed compositional analysis of the cylindrical precipitates revealed a pronounced and periodic modulation of the Co-concentration and, therefore, it was assumed that the formation of a new nucleus occurred preferentially in the [110] direction. Because of the pronounced anisotropy of elastic constants of copper there is an attractive elastic interaction between precipitates along the [110] direction.

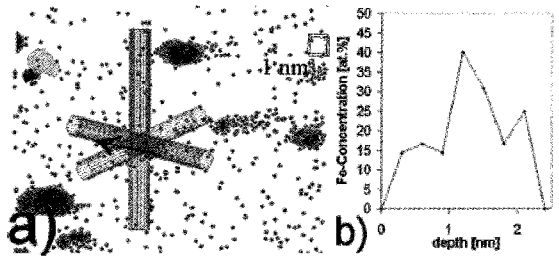

Figure 2 Distribution of Fe-atoms in a Cu-0.7 at.-% Fe alloy which was quenched into a homogeneous state and then annealed at 803 K for 5 min. One dimensional concentration profiles can be obtained in all directions, i.e. within the cylinders shown (a). The profile presented in b) is determined in the direction of the arrow shown in a).

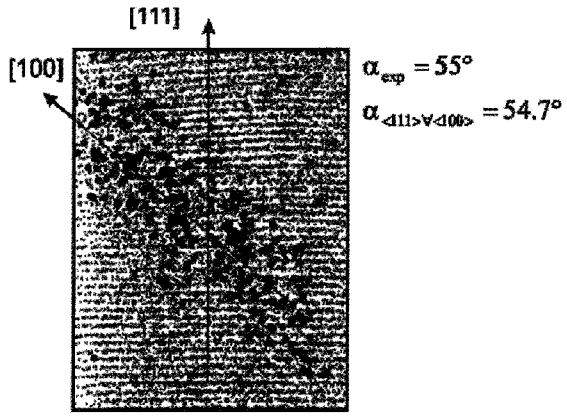

Figure 3 Positions of Cu-atoms (grey) and Ti-atoms (black and enlarged for clarity) in a Cu_3Ti precipitate in a Cu-0.7 at.-% Ti alloy annealed at 623 K for 30 days. The (111) Cu planes are going through the precipitate and, therefore, it has to be coherent.

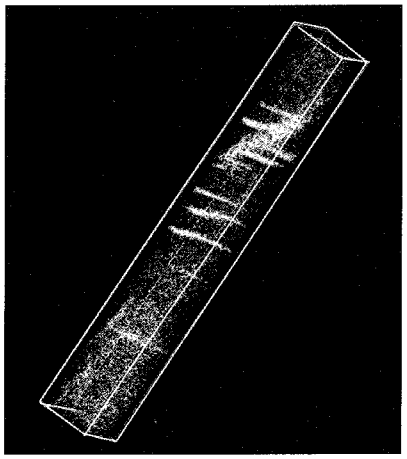

Figure 4 Position of Be-atoms in a Ni-12 at.-% Be alloy. Plate-like shaped precipitates can be observed.

2.2 Interdiffusion and interreaction at the boundary between two metals

In order to study the initial stages of interdiffusion or phase formation at the boundary between two metals, a special sample preparation technique has been developed (Ref. [6]). Tungsten

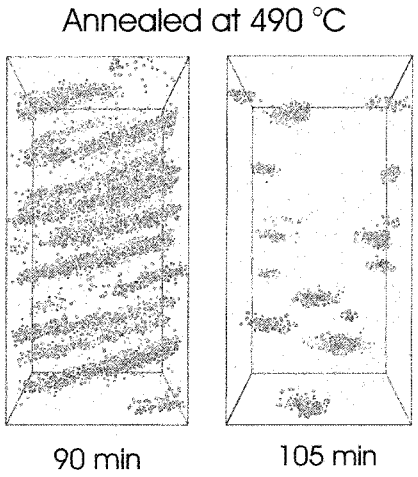

Figure 5 Position of Co-atoms in a Cu-2 at.-% Co alloy after annealing at the given temperature and time. Cylindrically shaped Co-precipitates form around 90 min and disappear a few minutes later.

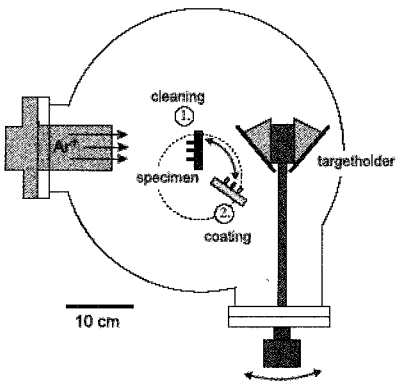

Figure 6 Sputtering apparatus (schematically) for cleaning tungsten tips by an ion argon gun (position 1) and depositing thin films onto the tip by sputtering from one or several targets (position 2).

tips were used as substrates, sputter cleaned in UHV and then covered with metal films by sputtering from a target (cf. Figure 6). This way double and multi layers could be produced in a clean way. It was essential to remove the natural oxide from the tungsten; otherwise the deposited metal films would not adhere properly and would be delaminated in the high electric fields during atom probe analysis.

It could be shown that the reaction between adjacent metals was very much controlled by the microstructure. In the presence of grain boundaries, diffusion occurred predominantly along the boundaries (cf. Figure 7 for silver reacting with aluminium). Boundaries became wetted this way and new phases formed in them. In the absence of grain boundaries sometimes new phases formed as closed layers at the border between the two metals (Ref. [7]). But in other cases isolated nuclei formed and grew by transport along their newly formed phase boundaries. A dense layer formed then by coalescence of all these particles (Ref. [8]).

2.3 P-segregation at grain boundaries in nanocrystalline Ni-P alloys,

Nickel-phosphorus alloys with varying P-content between 1 and 30 at.-% can be easily produced by chemical or electrochemical deposition from a solution. This way wear and corrosion resistant coatings are prepared in industry. It can be shown by X-ray and TEM analysis that alloys containing more than 15 at.-% P are amorphous whereas the ones with a lower P-content are nanocrystalline. It has been proved by 3-dimensional atom probe analysis of nanocrystalline Ni-3.6 at.-% P and -5.9 a.-% P (Ref. [9]) that the P-atoms are predominantly sitting in the grain boundaries. An example of the resulting inhomogeneous distribution of P-atoms is presented in Figure 8. In Figure 9 two slices from the analysed volume which are 1 nm thick, 10 nm wide and 170 nm long and which are perpendicular to each other intersecting in the middle of the analysed volume ($10\times10\times170\ nm^3$) the position of all the grain boundaries can be envisioned by presenting the P-enrichment. This way an average grain size was determined in excellent agreement with the broadening of Bragg peaks and TEM-results. The P-concentration in all grain boundaries was rather constant with an excess of about 1 Mol-P/m^2. Within the grains the P-concentration was reduced to about 1 at.-%. From a simple balance it could be shown (Ref. [9]) that

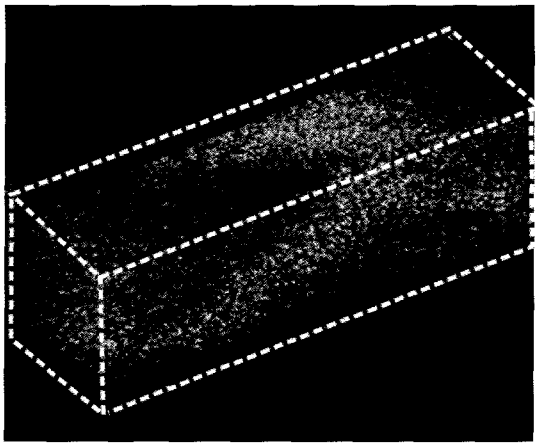

Figure 8 Distribution of P-atoms in a nanocrystalline Ni-3.6 at.-% P alloy ($10\times10\times60\ nm^3$). P-atoms segregate as 2-dimensional structures which are presumable grain boundaries (cf. Figure 9).

Figure 7 Position of Al-atoms (light grey) and Ag-atoms (dark grey) at the interface between the two metals after preparation by sputtering (left picture). The right picture reveals an interdiffusion of Al-atoms along the grain boundaries of silver after 15 min. at 100℃. No grain boundary was present in Al and, therefore, the reverse case of Ag-atoms diffusing into the grain boundaries of Al is not visible.

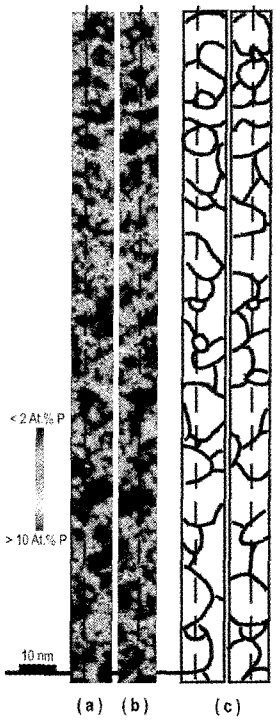

Figure 9 Left: varying P-concentration in a nanocrystalline Ni-3.6 at.-% P alloy presented in two perpendicular slices of the analysed volume (cf. text). Right: lines representing enrichment of phosphorus at grain boundaries. Thus the grain size can be compared with results obtained from analysing the broadening of X-ray diffraction peaks.

the grain boundary area increased with increasing P-content of the alloys or the grain size decreased, respectively. At 15 at.-% P it became less than 2 nm, i.e. below the detection limit of crystallinity by X-rays. Thus with increasing P-content more and more grain boundary regions had to be generated on the expense of grain regions, in order to accommodate the P-atoms. Finally, above 15% mostly all of the grain regions were consumed.

By annealing the nanocrystalline Ni-P alloys it turned out that they were rather stable with respect to grain coarsening. Remarkable grain growth was observed above 400 ℃ only, whereas pure nanocrystalline Ni coarsens around 200 ℃. In the light of Gibbs analysis (Ref. [10]) this effect was explained as a thermodynamic stabilization induced by grain boundary segregation (Ref. [11]). Gibbs concept developed for surfaces and grain boundaries was recently extended to other defects and segregation of solute atoms to these defects (Ref. [12]). This way the analysis of a special alloy provided insight to a rather general behaviour of the defect-solute interaction.

2.4 Thin oxide films in TMR-structures

Tunnelling magneto-resistance (TMR) structures are currently discussed as possible non-volatile memory devices. They are tri-layered structures with a thin (1 to 2 nm thick) oxide layer in between two magnetic materials. Because of spin polarized tunnelling of electrons through the oxide the resistance depends on the magnetic polarization of the adjacent magnetic films. An example of a cobalt/aluminium oxide/permalloy TMR-structure as it was analysed with the 3-dimensional atom probe is presented in Figure 10 (Ref. [13]). Despite the fact that aluminium oxide is an isolator and atom probe analysis is not possible with isolating materials, we succeeded in this case. Most probably charge transfer through the oxide, which is a requirement for removing atoms as ions from the sample tip, occurred by tunnelling in this case. For an oxide thickness above 2 nm higher voltages had to be applied to the tip and the sample fractured at the metal oxide interface.

Although the oxide was very thin, the atom probe analysis gave the expected composition of Al_2O_3. At the interface some intermixing occurred and even within the oxide iron and nickel from the permalloy were detected (cf. Figure 11).

2.5 Distribution of hydrogen in metallic multilayers

Hydrogen is very mobile in most metals and, therefore, it is able to be distributed in metallic multi layers at room temperature. For Fe/V-multi layers it has been shown by nuclear reaction analysis that hydrogen is accumulating in the vanadium layers (Ref. [14]). This is in agreement with the thermodynamic properties of the corresponding metal-hydrogen systems with vanadium having the higher affinity to hydrogen. However, V-layers with less than 1 nm thickness contained no hydrogen. This effect was explained by a so called "dead layer" at the V/Fe-interface due to "Fe-like" electrons spilling into vanadium and, therefore, reducing its affinity towards hydrogen. However, our atom probe analysis revealed (Ref. [15]) that not electrons but atoms were intermixing at the interface as shown in Figure 12. Instead of hydrogen deuterium was used because of a lower background signal. As deuterium behaves chemically like hydrogen no different results could be expected.

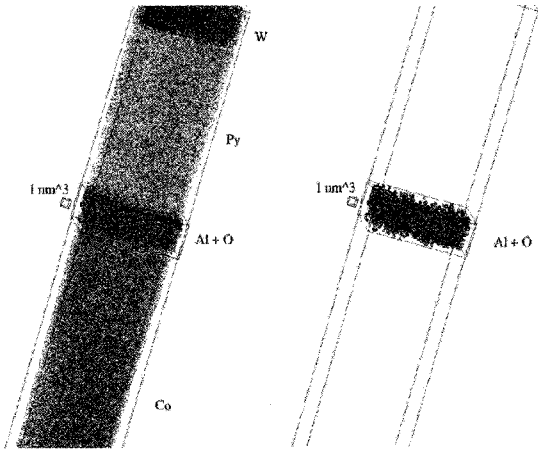

Figure 10 Atom distribution through a TMR structure deposited on a tungsten tip (upper part in the left hand picture). Adjacent to W followed a layer of permalloy (Ni and Fe) on top of that was an aluminium oxide layer of about 2 nm thickness. And finally a Co-layer was placed on top of the oxide. A compositional profile across this multilayered structure is shown in Figure 11.

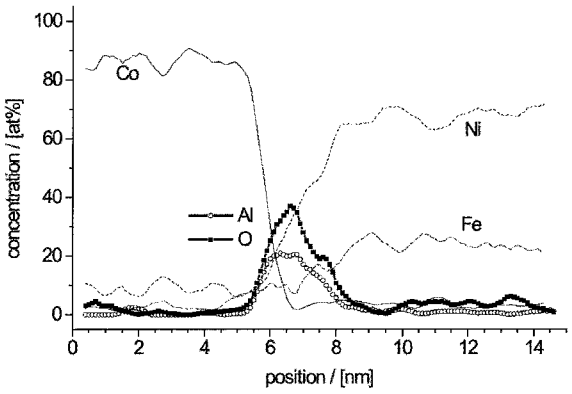

Figure 11 Concentration profile across a buried oxide layer of aluminium in between a Co-layer and permalloy (80% Ni and 20% Fe)

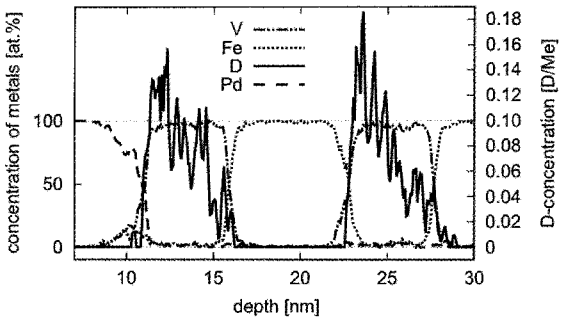

Figure 12 Concentration profile through Fe/V-multi layers and a Pd-cap (left, used for easy deuterium doping). Deuterium is enriched in the V-layers but avoids the regions of intermixing between Fe and V.

3 CONCLUSION AND OUTLOOK

The examples presented in chapter 2 reveal the enormous potential of an atom probe analysis. Although the number of laboratories using a 3-dimensional atom probe is increasing - with presently about 10 worldwide, the growth rate is rather small.

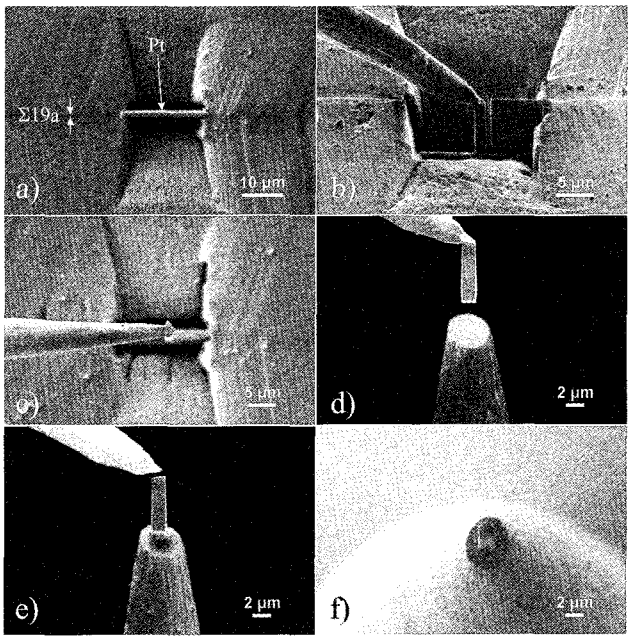

Figure 13 Focussed Ion Beam procedure for the preparation of a strip from a Cu-bicrystal doped with 50 atppm of Bi. a) the Σ19a grain boundary is protected with a Pt-layer and material is removed by ion milling above and below the boundary leaving a slice of the bicrystal, b) a strip is cut out of the slice by the ion beam and attached with platinum to the micro-manipulator, c) and d) the manipulator removes the strip and transports it to a blunt tungsten tip, e) the strip is welded to the W-tip by Pt-deposition and the manipulator is separated by the ion beam, e) top-view of the composite. In a following step the strip can be sharpened with the ion beam (cf. Figure 14).

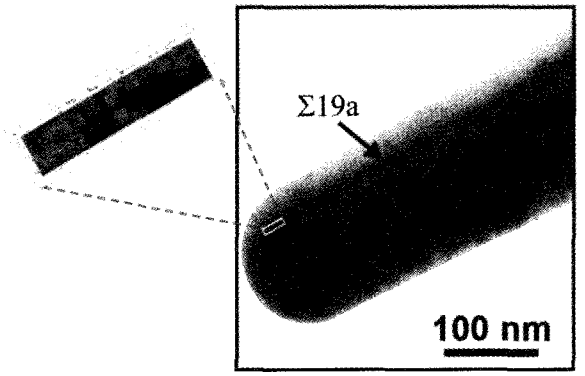

Figure 14 SEM-picture of the tip as prepared according to Figure 13 (right). The two grains adjacent to the Σ19a grain boundary are revealed by different contrast. The volume which has been analysed with the 3-dimensional atom probe is shown left. Within the analysed volume, i.e. within the grain boundary a Bi-enrichment was detected which corresponded to about half a monolayer.

There may be three reasons inhibiting a faster growth. First, the technique requires some experience in field ion microscopy. Second, it is restricted to conducting materials which are mostly metal and their alloys. Third, sample preparation is rather tedious as it is done by conventional electrochemical thinning which requires a lot of trial and error procedures.

Recent developments show that the second and third obstacle may be overcome rather easily. Regarding the second case, atom removal from tips can be achieved by laser pulses instead of high voltage pulses (Ref. [16]) and, therefore, samples could be isolators as well. The third problem can be solved by using a focused ion beam apparatus, where any sample shape can be produced by ion milling. This technique allows picking up certain regions of a sample and conducting an atom probe analysis in this region. An example is shown in Figure 13 (Ref. [17]), where a tip-shaped sample was prepared from a Σ19a {331} <110> grain boundary of a copper bicrystal which has been doped with about 50 atppm of bismuth. In order to do so, a slice containing the boundary was ion milled out of the bulk material. This is a conventional procedure for getting TEM specimen. Out of the slice a strip was cut by the ion beam and attached to a manipulator. In a following step the strip was welded to a tungsten tip and finally sharpened with the ion beam, in order to get the appropriate curvature for an atom probe analysis. The final specimen containing the grain boundary is presented in Figure 14. Analysing a part around the grain boundary with the atom probe revealed a strong segregation of Bi to this boundary.

Acknowledgement—The author is grateful for financial support by the Deutsche Forschungsgemeinschaft and the Volkswagenstiftung

References

[1] M. K. Miller, "*Atom Probe Tomography*", Kluwer Academic (2000)

[2] T. Al-Kassab, H. Wollenberger, G. Schmitz and R. Kirchheim in "*High-Resolution Imaging and Spectroscopy of Materials*", F. Ernst and M. Rühle eds., Springer Verlag 271-320 (2002)

[3] Heinrich, A., Al-Kassab, T., Kirchheim, R., "Investigation of the early stages of decomposition of Cu-0.7at.% Fe with the tomographic atom probe", Mater. Sci. Eng. A, 353, 92-98 (2003)

[4] Wolde-Georgis, D., Al-Kassab, T., Kirchheim, R. "Nucleation and growth in Cu-0.7at.% Ti as studied with the tomographic atom probe", Mat. Sci. Eng. A, 353, 152-157 (2003)

[5] Heinrich, Alexander, PhD thesis, University of Goettingen, (2005)

[6] Schleiwies, J. and Schmitz G., "Thin film interreaction of Al/Ag analyzed by tomographic atom probe", Materials Science and Engineering A, 327, 94-100 (2002)

[7] Jeske, T. Schmitz, G. and Kirchheim R.,"APFIM investigations of the early interreaction stages in Al/Ni-couples" Mat. Sci. Eng. A, 270, 64 (1999)

[8] Vovk, V., Schmitz, G., Kirchheim R., "Nucleation of product phase at reactive diffusion of Al-Co", Phys. Rev. B Phys. Rev. B, 69, 104102 (2004)

[9] Färber, B., Cadel, E., Menand, A., Schmitz, G., and Kirchheim, R., "Phosphorus Segregation in Nanocrystalline

Ni-3.6 at.-% P Alloys Investigated with the Tomographic Atomprobe (TAP)", Acta Mater. 48, 789 (2000)

[10] Gibbs, J.W., "The collected work of J.W. Gibbs", Vol. I, Longmans, Green and Co., New York 1928, p. 55

[11] Kirchheim, R., "Grain coarsening inhibited by solute segregation", Acta mater. 50, 413-419 (2002)

[12] Kirchheim, R., "Solid solutions of hydrogen in complex materials", In Solid State Physics, eds. H. Ehrenreich and F. Spaepen, Elsevier, Amsterdam, Vol. 59, 203-305 (2004)

[13] Kuduz, M., Schmitz, G., Kirchheim, R., "Investigation of oxide-tunnel barriers by atom probe tomography (TAP)", Ultramicroscopy 101, 197-205 (2004)

[14] Andersson, G., Hjörvarsson, B., and Isberg, P., Phys. Rev. B, 55, 1774 (1997)

[15] Kesten, P., Pundt, A., Schmitz, G., Weisheit, M., Krebs, H.U., and Kirchheim, R., "H- and D-distribution in metallic multilayers studied by 3-dimensional atom probe analysis and secondary ion mass spectrometry", JALCOM 330-332, 225-228 (2002)

[16] Vurpillot, F., Gilbert, M., Deconihout, B., "Towards the 3D FIM", Proceedings of the 49th International Field Emission Symposium, Graz, Austria, Surface and Interface Analysis, to be published

[17] Wolde_Georgis, Daniel, PhD thesis, University of Goettingen, (2005)